RSC Advances

ROYAL SOCIETY OF CHEMISTRY

www.rsc.org/advances

Journal Name

ARTICLE

One-pot synthesis and assembly of melamine-based nanoparticles for microporous polymer organic frameworks and its application as a support for silver nanoparticles catalyst

Received 00th January 20xx,
Accepted 00th January 20xx

DOI: 10.1039/x0xx00000x

www.rsc.org/

Xiaolong Zhao,*[a] Na Yan[b]

A facile solvothermal method was developed for one-pot synthesis of melamine-based nanoparticles and subsequent assembly to microporous polymer organic frameworks (POFs), without the aid of catalyst and template, using melamine and aromatic dialdehydes as the monomers. The structures and properties of the resulting materials were then systematically characterized by means of Fourier-transformed infrared (FTIR) spectroscopy, solid-state NMR, scanning electron microscopy (SEM) and N_2 adsorption isotherms. The results confirmed that nanoparticles were constructed firstly and then assembled to form porous structure with broad distribution of pore size and high surface areas, which is ideal for a balance between the mass-transportation and active sites. Given the solvothermal conditions of 180°C for 10 h, the as-prepared POFs possess intrinsic microporosity arisen from highly cross-linked aminal networks, with the specific surface areas of up to 718 m^2 g^{-1} and pore volume of up to 1.10 cm^3 g^{-1} at the molar ratio of 2:3 for melamine to terephthalaldehyde. The POFs supported silver nanoparticles shows an excellent catalytic performance for the degradation of methylene blue.

1. Introduction

Given their wide application in many important fields such as catalysis [1-3], gas storage [4,5], separation [6] and biomedicine [7,8], porous materials have received increasing attention in recent years. Various porous materials have been developed, including inorganic porous materials [9,10], metal-organic frameworks (MOFs) [11], covalent organic frameworks (COFs) [12-15], and polymer-based porous materials [16-18]. Polymer-based microporous materials are composed entirely of light elements (C, H, O, N, etc.) and linked through strong covalent bonds, exhibit low density, high thermal and/or chemical stability and might be a useful alternative of traditional inorganic porous materials. More importantly, there are numerous possibilities of pore size control and functionality tailoring for these materials through monomer selection and polymerization manipulation, these prominent features make them attractive candidates for myriad applications [19-22].

Polymer-based microporous materials with intrinsic porosity are usually formed by crosslinking of multiple functional building blocks with rigid or twisted structures. However, expensive and complex monomers are frequently used together with costly noble metal catalysts and/or harsh reaction conditions [16-18], which limit their widespread application. Therefore, great efforts are expected in the preparation of polymer organic framework (POF) materials based on cheap monomers and simple synthetic route. Melamine, a cheap and abundant chemical, has been used extensively in industries for plastics, paints, and paper production. A rigid triazine ring with three reactive amino groups, melamine is recognized as an ideal precursor for the fabrication of complex organic frameworks [23,24]. In addition, the feature of high nitrogen content (66% N by mass) has provided the resulting polymers with particular functionalities. Recently, Kailasam et al. synthesized the mesoporous melamine resins using block-co-polymer Pluronic F127 as the soft template, with the specific surface areas of up to 258 m^2 g^{-1} [25], while Schwab et al. developed a series of microporous polymer networks by reacting melamine with several aromatic di- and trialdehydes through Schiff base chemistry [26], by which a specific surface area up to 1377 m^2 g^{-1} was obtained. These materials were synthesized by long time refluxing (72 h) and yields of 61-66% were achieved. Subsequently, Han's group uses an alternative method via microwave irradiation to speed the reaction time to 4 h and

[a] Key Laboratory of Eco-Environment-Related Polymer Materials Ministry of Education; Key Laboratory of Polymer Materials of Gansu Province; College of Chemistry and Chemical Engineering, Northwest Normal University, Lanzhou, P. R. China 730070.

E-mail: zhaoxl82@nwnu.edu.cn

[b] Gansu Entry-Exit Inspection and Quarantine Bureau, Lanzhou, P. R. China 730020

E-mail: nianyue912@163.com

† Electronic Supplementary Information (ESI) available: Yields and Chemical elemental analysis of the melamined-based POFs; The XRD data and UV-Vis spectra of POF-M_2T_3/AgNPs composites; Fluorescence excitation and emission spectra of melamine, terephthalaldehyde and POF-M_2T_3; FTIR spectra of the melamine-based POFs prepared with different M/T ratios or M/I ratios; Rotating 3D structure model for POF-M_2T_3 and POF-M_2I_3; FTIR spectra of melamine, terephthalaldehyde and POF-M_2T_3; FTIR spectra of melamine, isophthalaldehyde and POF-M_2I_3; SEM image of POF-M_4T_3 and POF-M_4I_3; Nitrogen adsorption and desorption isotherm of POF-M_4T_3 and POF-M_4I_3; Thermogravimetric analysis of POF-M_2T_3, POF-M_4T_3, POF-M_2I_3 and POF-M_4I_3; Successive UV-vis absorption spectra of the reduction of methylene blue. See DOI: 10.1039/x0xx00000x

improve the yields up to 90%, but the microwave assisted synthesis leads to decrease in porosity as well as specific surface area (301 m^2 g^{-1}) [27]. These successful examples indicated that reaction condition plays an important role on the properties of the final microporous materials while it remains a great challenge to develop simple and catalyst-free synthesis methods for their large-scale fabrication.

On the other hand, although the materials with nano or mesopores might provide very high surface areas, the use of these surfaces could be hindered by the small pore sizes. Presence of larger pores is therefore critical for the efficient use of all porous surfaces. Using porogen is the traditional way to implement bigger pores but subsequent removal of these agents must be preformed. Recently, there are some works proved that assembly of nanoparticles was another efficient way to form porous materials, the resulting pore sizes were dependent on the starting nanoparticles [28,29]. Successful examples are mainly inorganic, but a two stage mechanism including the formation of colloidal dispersions and subsequent assembly to organic networks has been reported [30]. It can be expected that this strategy is extremely useful to build porous materials from organic nanoparticles with nanopores, to get both high surface area and good accessibility of the inner pores.

Solvothermal synthesis is a versatile method used in the preparation of inorganic nanocrystals with special performance [31,32]. In our attempt to synthesize nanoparticles using melamine and dialdehydes, it was found that prolonged treatment of the nanoparticle solutions might give nice porous solids. Herein, a facile one-pot solvothermal synthesis of microporous POFs through assembly of nanoparticles from solution of melamine and aromatic dialdehydes was proposed (Scheme 1). Without the aid of catalyst and template, POFs were prepared using melamine and terephthalaldehyde as the monomers with the specific surface areas of up to 718 m^2 g^{-1} and pore volume of up to 1.10 cm^3 g^{-1}. Similar with the two stage organic sol-gel synthesis [30], the method involves the formation of nanoparticles with pore sizes at the molecular length scales, and the assembly of nanoparitlces to form much bigger pores, but these two steps were realized in a single heating within a relatively short period of time. Subsequently, silver nanoparticles were supported onto the POFs for the degradation of methylene blue, a cationic thiazine dye commonly used as a model compound to evaluate the efficiency of an adsorbent or a catalyst for removing the dyes from aqueous solution [33,34].

2. Materials and methods

2.1. Materials

Melamine (M, 99%) was obtained from Shanghai Shiyi Chemical Reagent (Shanghai, China). Terephthalaldehyde (T, 99%), isophthalaldehyde (I, 97%), methylene blue (MB, 97%), sodium borohydride ($NaBH_4$, 99.9%) and silver nitrate ($AgNO_3$, 99%) were received from Sigma-Aldrich. Dimethyl sulfoxide (DMSO, 99%) was purchased from Tianjin Guangfu Fine Chemical Research Institute (Tianjin, China). All chemicals were of analytical reagent grade and used without further purification.

2.2. Synthesis of melamine-based microporous polymer organic frameworks

Melamine-based microporous polymer organic frameworks were synthesized via a versatile solvothermal method. Typically, melamine (470 mg, 3.73 mmol) and terephthalaldehyde (750 mg, 5.59 mmol) were dissolved in DMSO (23 mL) to form a clear solution with the assistance of ultrasound in a hot bath. Subsequently, the mixture was transferred into a Teflon-lined autoclave (100 mL capacity) and heated to and maintained at 180°C for 10 h. After cooled down to room temperature, the reaction mixture was filtered over a Büchner funnel, and the precipitated solid was successively washed with excess acetone (30 mL×2) and dichloromethane (30 mL×2). The as-obtained white powders were then dried under vacuum at room temperature for 10 h. In this step, the molar ratio of melamine (M) to terephthalaldehyde (T) was 2:3, and the obtained polymer organic frameworks were named POF-M_2T_3. In the similar procedure, other POFs were obtained by changing terephthalaldehyde into isophthalaldehyde or varying molar ratio of melamine to terephthalaldehyde or isophthalaldehyde. The obtained POFs with the yields were shown in Supplementary Table S1, and characteristic elemental analysis shown in Supplementary Table S2.

2.3. Preparation of POF-M2T3 supported silver nanoparticles (AgNPs) catalyst

Under stirring, 4.6 mL stock solution of 0.01 mol L^{-1} $AgNO_3$ was added into 100 mL distilled water, while 100 mg POF-M_2T_3 was immersed and stirred for 2 h. Then, a freshly prepared $NaBH_4$ solution (2.3 mL, 0.1 mol L^{-1}) was added into above mixture and kept for 2 h in order to reduce the silver ions into silver nanoparticles. After filtration, the product was washed with distilled water for three times, dried in vacuum at 45°C for 10 h, and marked as POF-M_2T_3/AgNPs. The sample was digested in *aqua regia* and the silver percentage was determined by an IRIS Advantage ER/S inductively coupled plasma atomic emission spectrometer (Thermo Jarrel Ash, Franklin, MA, USA).

2.4. Characterization

Fourier-transformed infrared (FTIR) spectra were collected on a Thermo Nicolet NEXUS TM spectrophotometer using KBr pellets. Solid-state NMR experiments were performed on a Bruker WB Avance II 400 MHz spectrometer. The ^{13}C CP/MAS NMR spectra were recorded with a 4 mm double resonance probe with a sample spinning rate of 10 kHz. The elemental analyses were performed on a Vario EL elemental analyzer (Elementar, Germany). Scanning electron microscopy (SEM) images were obtained using a Hitachi S-4800 field emission scanning electron microscope with an accelerating voltage of 5 kV. Finely ground sample was prepared for analysis by dispersing onto a flat aluminum sample holder, and then coated with a gold film to facilitate conduction using an E-1045 sputter coater. The nitrogen adsorption and desorption isotherms were measured at 77 K using a Micromeritics ASAP 2020M system. The samples were outgassed at 150°C for 5 h

before the measurements. The specific surface areas for N_2 were calculated using the Brunauer-Emmet-Teller (BET) model. The pore size distributions were calculated from the adsorption isotherms by Barrett-Joyner-Halenda (BJH) model. Thermal gravimetric analysis (TGA) measurements were examined using a Linseis-STA PT1600 thermal analyzer (Linseis Scientific Instruments, Germany) at a heating rate of 5°C/min under nitrogen flow. The morphologies and particle sizes of the POF-M_2T_3/AgNPs catalysts were characterized by a JEOL JEM-2010 transmission electron microscope operated at 200 kV. Powder X-ray diffraction (XRD) patterns were performed on a PANalytical X'Pert Pro X-ray diffractometer carried out at 40 kV and 40 mA with Cu Kα radiation (λ=1.54056 Å). Fluorescence spectra were obtained on a RF-5301PC spectrofluorophotometer (Shimadzu), using 5 nm slit width for both excitation and emission. The mean hydrodynamic particle size was determined in DMSO by dynamic laser light scattering (BI-200SM, Brookhaven Instruments).

2.5. Catalytic experiment

The methylene blue (MB) reduction reaction using POF-M_2T_3/AgNPs as the catalyst was studied by dispersing the POF-M_2T_3/AgNPs composites in a MB solution. Firstly, the stock solutions of the dye and reducing agent were purged with nitrogen gas for 10 min to remove dissolved oxygen before use. After that, 200 mg POF-M_2T_3/AgNPs was dispersed in a solution containing 20 mL 0.005 mol L^{-1} of MB solution and 10 mL 0.1 mol L^{-1} of $NaBH_4$ solution. Immediately, the progress of the reaction was monitored at an interval of 2 min using a TU-1901 double beams UV-Vis spectrophotometer (Beijing Purkinje General Instrument, China).

3. Results and discussion

3.1. Synthesis of melamine-based porous polymer organic frameworks

To verify the polymer structure, the molar ratio of melamine to terephthalaldehyde was investigated on five different levels: 1:3, 2:3, 3:3, 4:3 and 5:3 (melamine:terephthalaldehyde, M:T), in which the amount of melamine was gradually increased with different molar ratio. For all molar ratios studied, nanoparticles formed within 2 h and microporous POFs were obtained with extended reaction time under solvothermal synthesis condition (180°C, 10 h). As shown in Fig. 1a, the diameter of nanoparticles formed at the initial stage is ~1 nm, with unique UV-Vis absorption and fluorescence characteristics (Supplementary Fig. S1 and S2). With prolonged reaction time, nanoparticles assembled into 3D network and POFs formed. FTIR spectra demonstrate that no absorption bands attributable to imine (-C=N-) stretching vibration around 1600 cm^{-1}, and also, with increasing the molar ratio of melamine to terephthalaldehyde, no visible differences are impressive except for the absorption intensities (Supplementary Fig. S3). Similar results have been obtained when isophthalaldehyde was used instead of terephthalaldehyde (Supplementary Fig. S4). Although melamine coupling with phthalaldehyde may theoretically form two kinds of bonds, imine (-C=N-) with an ideal ratio of M:T of 2:3 and aminal (-HN-C-NH-) with an ideal ratio of M:T of 4:3, these spectral features apparently indicate the formation of aminal networks between amino and aldehyde groups, regardless of the molar ratio of reactants. This result agrees with that obtained by Schwab et al. at M:T of 2:3, and they proposed that the imine double bonds might be subsequently attacked by primary amines to generate aminals [26]. However, the molar ratio of melamine and aromatic dialdehydes will produce a great influence on the specific surface area, porosity and yield for the polymer networks. For both polymer networks prepared by terephthalaldehyde and isophthalaldehyde, these properties at the molar ratio of 2:3 are superior to those at 4:3 (Table 1). And the polymer networks with terephthalaldehyde as the monomer exhibits higher surface area than that with isophthalaldehyde as the monomer, presumably as a result of steric effect (Supplementary Fig. S5 and S6). So further characterization and application for this type of polymer focused on that obtained with M:T of 2:3.

3.2. Structure analysis of melamine-based porous polymer organic frameworks

In FTIR (Fig. 2), the absorption bands at 3469 and 3419 cm^{-1} (NH_2 stretching) and 1652 cm^{-1} (NH_2 deformation), which are attributable to primary amine group of melamine, have disappeared or drastically reduced after the reaction. Simultaneously, the main spectral featured absorption bands attributed to aromatic dialdehydes at around 2870 cm^{-1} (C-H stretching) and 1695 cm^{-1} (C=O stretching) are absent in the spectra of polymer materials (Supplementary Fig. S7 and S8). The absence or decrease in the absorption intensities of these bands is an indication of a successful dehydration reaction between the amino and aldehyde groups. In addition, the structures of the triazine ring give the strong stretching vibration bands at 1547 and 1479 cm^{-1} (C=N vibration), mirroring the successful incorporation of the melamine into the framework, while the absence of characteristic band at around 1600 cm^{-1} due to imine linkages (Ar-C=N stretching vibration) indicates that an alternative bond, i.e. aminal group (HN-C-NH), dominates the whole polymer networks. Solid-state ^{13}C CP/MAS NMR was further utilized to characterize the polymer structure (Fig. 3). The strong resonance at 166 ppm is assigned to the aromatic carbons of the triazine ring of melamine, and the signals at 129 and 136 ppm are correlated to aromatic carbons of the benzene ring. The resonance at 54 ppm corresponds to the carbon atoms in aminal units, as a result of the reaction between amino and aldehyde groups. No C=N resonance at 160 ppm is observed, indicating the absence of imine bond in the polymer networks, whereas the disappearance of resonance peak at 194 ppm reflects no unreacted aldehyde groups in the product, consistent with FTIR analysis. In addition, residual DMSO in the polymer is responsible for the signal at 39 ppm.

To investigate the microstructure of the melamine-based POFs, four samples with different monomers and composition ratios were characterized by SEM (Fig. 1, Supplementary Fig. S9 and S10). All SEM images show similar morphologies, rendering

that nicely shaped nanoparticles assemble to form "cauliflower-type" morphology. The porous properties of these polymer materials were analyzed by N_2 adsorption-desorption isotherms (Fig. 4, Supplementary Fig. S11 and S12), and the results are summarized in Table 1. At low relative pressures, a high uptake of nitrogen is observed, representing the microporous nature of the polymer networks. At higher pressures (P/P_0>0.9), the steep upward-sloping trend of the isotherms indicates the presence of larger pores, which originate from the interparticle porosity, i.e. interspace of the assembled nanoparticles. Furthermore, the minimal hysteresis in these profiles suggests that the adsorption and desorption are equally facile, this characteristic shared by all POFs studied. As listed in Table 1, the polymer POF-M_2T_3 has the highest Brunauer-Emmet-Teller (BET) surface area of 718 m^2 g^{-1} and pore volume of 1.10 cm^3 g^{-1}, while with increasing the molar ratio of melamine to dialdehyde results in a decrease of specific surface area to 642 m^2 g^{-1} and pore volume to 0.72 cm^3 g^{-1}. Presumably, higher melamine content brings in more unreacted -NH_2 groups, which are easy to form hydrogen bonds between the melamine-based molecules, leading to the decrease in porosity as well as specific surface area [27]. A similar relation between monomer structure and resulting porosity has also been observed for the POFs derived from the monomers of isophthalaldehyde and melamine, though these values are lower than those obtained from terephthalaldehyde. According to the pore size distribution curves (inset of Fig. 4), the POFs show predominant presence of both micropores and mesopores, with the BJH average pore width of ~12.0 nm (Table 1). However, although significant difference in surface area was observed, it is hard to distinguish the difference in the porosity between the POFs obtained with various dialdehydes from the SEM images. It can be reasonablely deduced that the difference of the surface area mainly comes from the nanopores inside the nanoparticles. As a rough evaluation, the surface area comes from the agglomeration of the nanoparticles is around 375 m^2 g^{-1} if assuming these nanoparticles are spherical shape with a diameter of ~ 40 nm (taken from Fig. 1b) and a specific bulk density of 0.4 g cm^{-3} [35]. Approximately 52% of surface area comes from the outer surface of nanoparticles. Therefore, the practical way of increasing the surface area of the final material depends on the structure of the nanoparticles. Because the structure of nanoparticles can be feasibly tuned through the synthesis conditions, there is great potential to synthesis various POFs using the proposed route. Although the surface areas are somewhat lower than that reported by Schwab et al. [26], it is still a practical method to obtain catalyst carrier because of the simple operations and fast preparation process. Also, there are plenty of possibilities of further improvement by fine tune of solvothermal protocols. Even under the present conditions, the specific surface area is already superior to other melamine-based POFs [25,27,35-39].

Subsequent TGA analysis exhibits a limited weight-loss before 350°C, suggesting their excellent thermal stability of all POFs (Supplementary Fig. S13). Preliminary solubility experiments show that the obtained melamine-based POFs are insoluble in all organic solvents tested including methanol, acetone, tetrahydrofuran, N,N-dimethyl formamide, dichloromethane, DMSO and hexane, as well as water and alkaline solution. Slight solubility in inorganic strong acid such as concentrated H_2SO_4 and HNO_3 was observed, possibly due to the breakage of links between some nanoparticles. These characters make these POFs promising as good candidates of catalyst carriers in harsh environment. Furthermore, these POFs are convenient for recycling of loaded noble metal catalysts because the POFs can completely decomposed simply by heating over 600°C (Supplementary Fig. S13).

3.3. Characterization of POF-M_2T_3/AgNPs composites

To verify its applicability, silver nanoparticles supported on POF-M_2T_3 were prepared using a simple impregnation and reduction method in which $NaBH_4$ could not affect the stability of the POF-M_2T_3 and could reduce the silver ions into silver nanoparticles exclusively. ICP-AES analysis results showed that the average Ag percentage was 1.39 wt% for the as-prepared POF-M_2T_3/AgNPs catalyst. From TEM images (Fig. 5a), AgNPs were uniformly embedded within the polymer networks, with the size of ~10 nm. Subsequently, XRD pattern of the POFs (Fig. 5a) demonstrated some featured diffraction peaks at 2θ values of 38.2°, 44.5°, 64.6°, and 77.5°, corresponding to (111), (200), (220) and (311) crystal planes of silver particles. The calculated d-spacing was in accordance with that of the International Centre for Diffraction Data obtained from JCPDS files (No. 41-1402), suggesting that the AgNPs have a structure of cubic symmetry (Supplementary Table 3) with the average particle size of 8.2 nm.

3.4. Catalytic degradation of MB

The catalytic activity of the as-prepared catalyst was evaluated via the degradation of methylene blue (MB). Fig. 5b records the UV-Vis spectra with the reduction time at an interval of 2 min. It is clearly observed that with the addition of the catalyst, the characteristic absorbance at 665 nm was gradually decreased and gets unchangeable after 12 min for MB solution. During this process, the blue color of MB solution faded quickly, and finally bleached (Fig. 5b), while with the addition of equal amount of POF material into the MB solution did not cause any evident color change after 1 h. This fact suggests effective activity of the catalyst for the degradation of MB. The reusability was investigated using the same catalyst after a simple centrifugation and washing with distilled water. The results indicate that by consecutive seven cycles, the catalytic activity of the composite shows no obvious decrease (Supplementary Fig. S14). Also, it is noticeable that there is no characteristic absorption peak at around 420 nm for both reaction and washing solutions, revealing that there has been no leakage of AgNPs from the POFs, probably due to the high affinity of N atoms to Ag nanoparticles.

Conclusions

In summary, we have developed a facile one-pot route for microporous POFs through assembly of organic nanoparticles using melamine and aromatic dialdehydes. Using typical solvothermal method, nanoparticles was firstly formed and,

POFs was obtained with prolonged reaction time. Systematic characterizations demonstrate that with the dehydration reaction between the amino and aldehyde groups, aminal bonds are predominant within the polymer networks. Using melamine and terephthalaldehyde as the monomers, this thermally stable polymer presents the specific surface areas of up to 718 $m^2 g^{-1}$ and pore volume of up to 1.10 $cm^3 g^{-1}$. The obtained POFs possess purely organic framework with a nitrogen content of up to 40 wt%. They also have large specific surface areas and high thermal/chemical stability. The proposed solvothermal synthetic protocol forming micropores both inside individual nanoparticles and the interspace between the assembled nanoparticles, therefore provides one-pot facile catalyst-free and template-free synthesis. The extra benefit of this dual-modal structure is that interspace between the nanoparticles can act as the 'trunk road' and facilitate the transportation of molecules to and from the nanopores spreading inside nanoparticles either as catalyst carriers or adsorbents. When the carrier role is applied, the POFs can entrap more Ag nanoparticles for catalytic degradation of methylene blue and consecutive seven cycles reveal the stable catalytic activity of the composite during the catalytic process.

Acknowledgements

We thank the financial support from the National Nature Science Foundation of China (Grant 21462039), the Natural Science Foundation of Gansu Province (Grant 1308RJZA103), and the Ability-Promoted Program of Young Teacher in Northwest Normal University (Grant NWNU-LKQN-12-1).

Notes and references

1 D. E. De Vos, M. Dams, B. F. Sels, P. A. Jacobs, *Chem. Rev.*, 2002, **102**, 3615.
2 J. Lee, O. K. Farha, J. Roberts, K. A. Scheidt, S. T. Nguyen, J. T. Hupp, *Chem. Soc. Rev.*, 2009, **38**, 1450.
3 M. Yoon, R. Srirambalaji, K. Kim, *Chem. Rev.*, 2012, **112**, 1196.
4 R. E. Morris, P. S. Wheatley, *Angew. Chem. Int. Edit.*, 2008, **47**, 4966.
5 M. P. Suh, H. J. Park, T. K. Prasad, D. W. Lim, *Chem. Rev.*, 2012, **112**, 782.
6 J. R. Li, J. Sculley, H. C. Zhou, *Chem. Rev.*, 2012, **112**, 869.
7 A. C. McKinlay, R. E. Morris, P. Horcajada, G. Férey, R. Gref, P. Couvreur, C. Serre, *Angew. Chem. Int. Edit.*, 2010, **49**, 6260.
8 P. Horcajada, R. Gref, T. Baati, P. K. Allan, G. Maurin, P. Couvreur, G. Férey, R. E. Morris, C. Serre, *Chem. Rev.*, 2012, **112**, 1232.
9 J. Jiang, J. Yu, A. Corma, *Angew. Chem. Int. Edit.*, 2010, **49**, 3120.
10 Y. Shi, Y. Wan, D. Zhao, *Chem. Soc. Rev.*, 2011, **40**, 3854.
11 N. Stock, S. Biswas, *Chem. Rev.*, 2012, **112**, 933.
12 H. M. El-Kaderi, J. R. Hunt, J. L. Mendoza-Cortés, A. P. Côté, R. E. Taylor, M. O'Keeffe, O. M. Yaghi, *Science*, 2007, **316**, 268.
13 F. J. Uribe-Romo, J. R. Hunt, H. Furukawa, C. Klöck, M. O'Keeffe, O. M. Yaghi, *J. Am. Chem. Soc.*, 2009, **131**, 4570.
14 F. J. Uribe-Romo, C. J. Doonan, H. Furukawa, K. Oisaki, O. M. Yaghi, *J. Am. Chem. Soc.*, 2011, **133**, 11478.
15 T. E. Reich, S. Behera, K. T. Jackson, P. Jena, H. M. El-Kaderi, *J. Mater. Chem.*, 2012, **22**, 13524.
16 P. M. Budd, N. B. McKeown, D. Fritsch, *J. Mater. Chem.*, 2005, **15**, 1977.
17 N. B. McKeown, P. M. Budd, *Macromolecules*, 2010, **43**, 5163.
18 A. Thomas, *Angew. Chem. Int. Edit.*, 2010, **49**, 8328.
19 N. B. McKeown, P. M. Budd, *Chem. Soc. Rev.*, 2006, **35**, 675.
20 J. Germain, J. M. J. Fréchet, F. Svec, *Small*, 2009, **5**, 1098.
21 A. Thomas, P. Kuhn, J. Weber, M. M. Titirici, M. Antonietti, *Macromol. Rapid. Comm.*, 2009, **30**, 221.
22 P. Kaur, J. T. Hupp, S. T. Nguyen, *ACS Catal.*, 2011, **1**, 819.
23 M. B. Steffensen, E. Hollink, F. Kuschel, M. Bauer, E. E. Simanek, *J. Polym. Sci. Part A: Pol. Chem.*, 2006, **44**, 3411.
24 T. J. Mooibroek, P. Gamez, *Inorg. Chim. Acta.*, 2007, **360**, 381.
25 K. Kailasam, Y.-S. Jun, P. Katekomol, J. D. Epping, W. H. Hong, A. Thomas, *Chem. Mater.*, 2010, **22**, 428.
26 M. G. Schwab, B. Fassbender, H. W. Spiess, A. Thomas, X. Feng, K. Müllen, *J. Am. Chem. Soc.*, 2009, **131**, 7216.
27 G. Yang, H. Han, C. Du, Z. Luo, Y. Wang, *Polymer*, 2010, **51**, 6193.
28 C. B. Murray, C. R. Kagan, M. G. Bawendi, *Annu. Rev. Mater. Sci.*, 2000, **30**, 545.
29 Y. Tao, H. Kanoh, L. Abrams, K. Kaneko, *Chem. Rev.*, 2006, **106**, 896.
30 S. Y. Moon, J. S. Bae, E. Jeon, J. W. Park, *Angew. Chem. Int. Edit.*, 2010, **49**, 9504.
31 R. I. Walton, *Chem. Soc. Rev.*, 2002, **31**, 230.
32 D. R. Modeshia, R. I. Walton, *Chem. Soc. Rev.*, 2010, **39**, 4303.
33 M. Azarang, A. Shuhaimi, R. Yousefi, S. P. Jahromi, *RSC Adv.*, 2015, **5**, 21888.
34 Z. Lu, X. Xiang, L. Zou, J. Xie, *RSC Adv.*, 2015, **5**, 42580.
35 M. G. Schwab, D. Crespy, X. Feng, K. Landfester, K. Müllen, *Macromol. Rapid. Comm.*, 2011, **32**, 1798.
36 A. Deryło-Marczewska, J. Goworek, S. Pikus, E. Kobylas, W. Zgrajka, *Langmuir*, 2002, **18**, 7538.
37 C. du Fresne von Hohenesche, D.F. Schmidt, V. Schädler, *Chem. Mater.*, 2008, **20**, 6124.
38 Y. Luo, B. Li, L. Liang, B. Tan, *Chem. Commun.*, 2011, **47**, 7704.
39 A. Wilke, J. Weber, *J. Mater. Chem.*, 2011, **21**, 5226.

Table 1

Composition and pore characteristics of the melamine-based POFs.

Samples	Molar ratio[a]	S_{BET}[b] ($m^2\ g^{-1}$)	V_{total}[c] ($cm^3\ g^{-1}$)	V_{micro}[d] ($cm^3\ g^{-1}$)	d_{pore}[e] (nm)
POF-M_2T_3	2:3	718	1.1	0.2	12
POF-M_4T_3	4:3	642	0.72	-[f]	7.7
POF-M_2I_3	2:3	474	0.93	0.09	11.3
POF-M_4I_3	4:3	235	0.34	-[f]	7.8

[a] Molar ratio of Melamine (M) to terephthalaldehyde (T) or isophthalaldehyde (I). [b] Specific surface area calculated from nitrogen adsorption isotherms using the BET equation. [c] Pore volume calculated from nitrogen adsorption at p/p_0=0.99. [d] Micropore volume calculated from nitrogen adsorption at p/p_0=0.1. [e] BJH average pore diameter calculated from desorption data. [f] N/A: Not applicable.

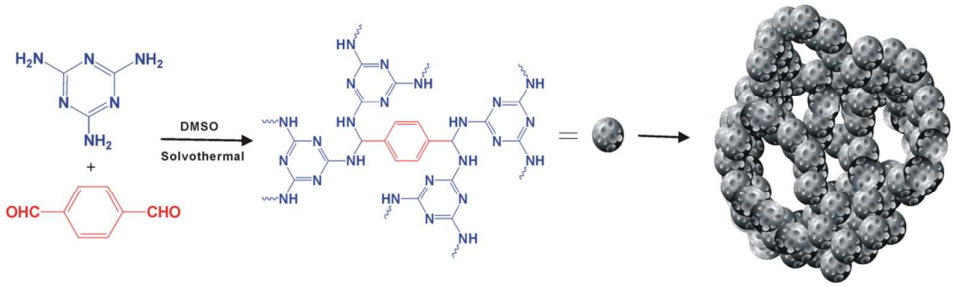

Scheme 1. Structure and schematic illustration of melamine-based microporous polymer organic frameworks.

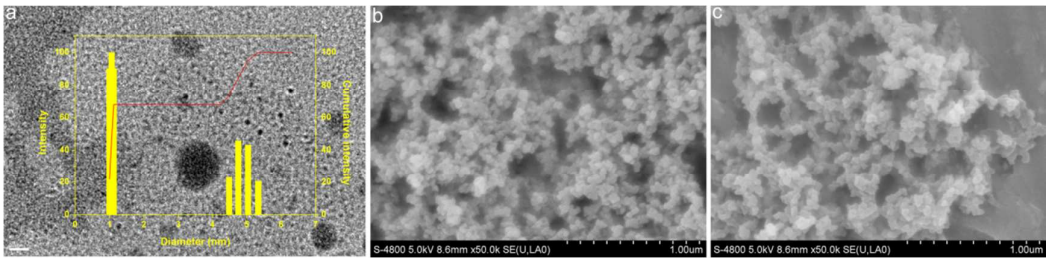

Fig. 1. TEM micrograph (Bar = 20 nm) and hydrodynamic particle size distribution of POF-M_2T_3 (reaction for 2 h) in DMSO measured by dynamic laser light scattering (a); SEM images of POF-M_2T_3 (b) and POF-M_2I_3 (c) with the reaction time of 10 h.

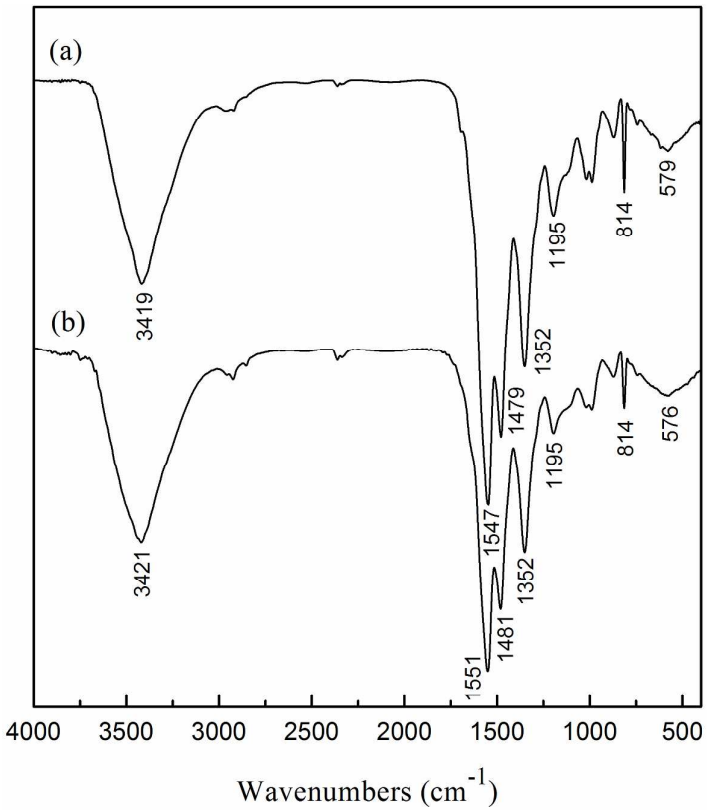

Fig. 2. FTIR spectra of POF-M_2T_3 (a) and POF-M_2I_3 (b).

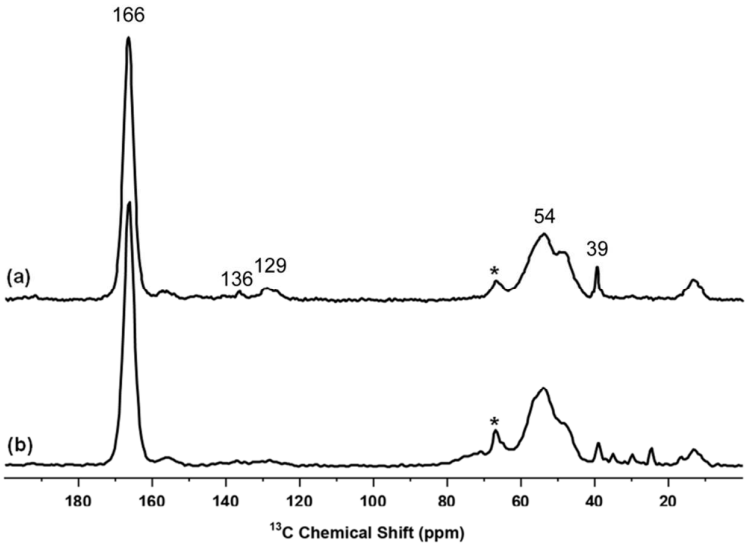

Fig. 3. ^{13}C CP/MAS NMR spectra of POF-M_2T_3 (a) and POF-M_2I_3 (b). Asterisks denote spinning sidebands.

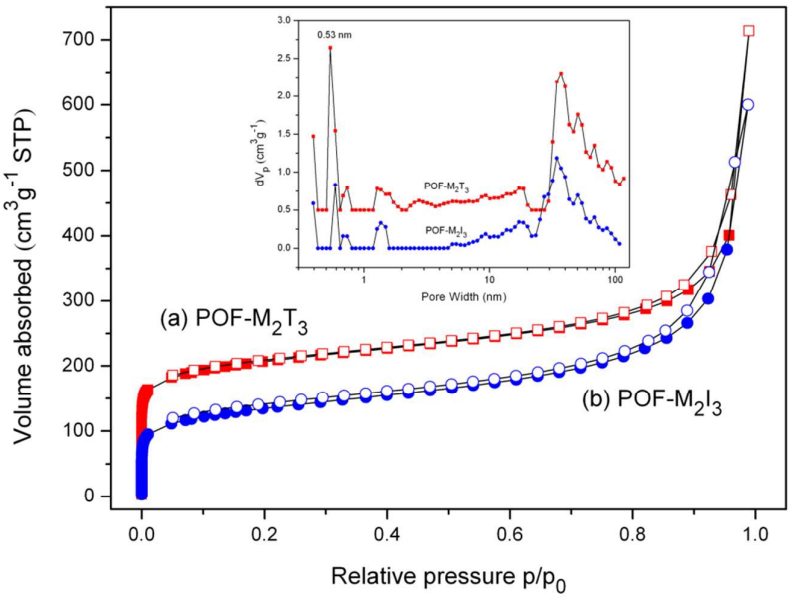

Fig. 4. Nitrogen adsorption (filled symbols) and desorption (empty symbols) isotherms of POF-M_2T_3 (a) and POF-M_2I_3 (b). Inset: Pore size distribution of POF-M_2T_3 and POF-M_2I_3.

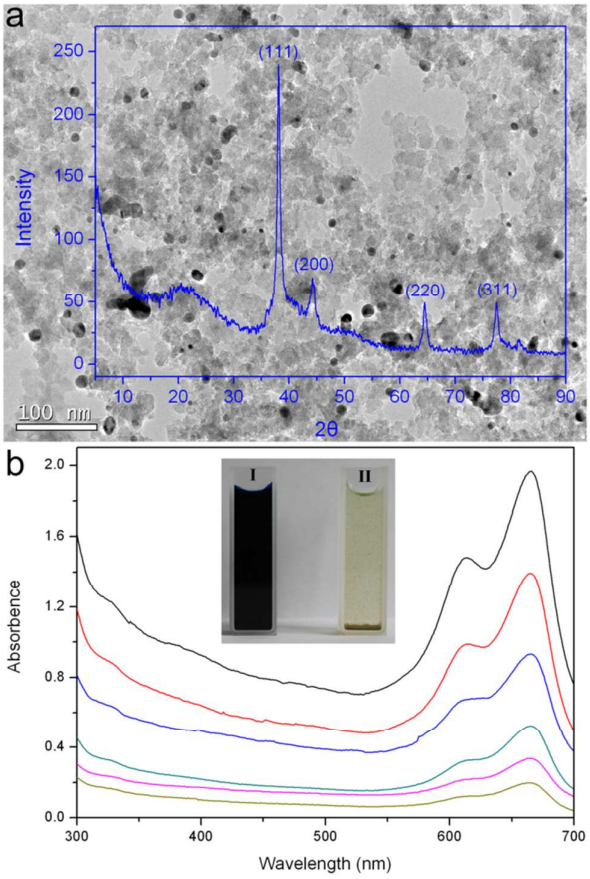

Fig. 5. (a) TEM micrograph and XRD pattern of POF-M_2T_3/AgNPs composites; (b) Successive UV-Vis absorption spectra of the reduction of methylene blue by $NaBH_4$ in the presence of POF-M_2T_3/AgNPs composites. From the top to the bottom, UV-Vis spectra of 2-12 min with an interval of 2 min, in which the insets show the photographs of MB solution without (I) and with (II) the POF-M_2T_3/AgNPs composites after 12 min.

A facile one-pot route was developed to obtain organic nanoparticles for fabrication of microporous POFs using melamine and aromatic dialdehydes as the starting materials. The POFs possess intrinsic microporosity and, the micropore size and its distribution can be tuned simply at either the nanoparticle forming and nanoparticle growing and assembling stage. The as-prepared POFs can be utilized as the support to entrap Ag nanoparticles and the resulting Ag^0-loaded POFs show excellent catalytic performance for organic dyes in water, such as methylene blue in this study.